Pure Appl. Chem., Vol. 81, No. 3, pp. 549–570, 2009.
doi:10.1351/PAC-CON-08-08-24

Conformational symmetry and vibrational dynamics of polymers*

Poonam Tandon‡, Naresh Kumar, Vineet Gupta, Deepika Chaturvedi, Soni Mishra, and Vishwambhar D. Gupta

Department of Physics, University of Lucknow, Lucknow 226 007, India

Abstract: Polymers are an important class of materials, and their conformation dictates their dynamical, thermodynamical, and hydrodynamical behavior. Several spectroscopic and other techniques have been employed to characterize their conformation. However, little use has been made of group-theoretical techniques except in the classification of symmetry species. In the present review, an attempt has been made to correlate normal modes and their dispersion profiles with the conformation of the polymeric systems. This has been attempted in the case of 2-, 3-, 4-fold and α-helical polymers.

Keywords: polymers; conformation; dispersion curves; heat capacity; density of states; vibrational spectra.

INTRODUCTION

Polymers are important structural units of living and non-living systems, each by itself, often exercising surprising and complicated functions. Polymers consist of chains built up from a relatively small number of different types of monomer units. The most important of these polymers are proteins, which include enzymes that catalyze and regulate metabolism and the nucleic acids, which carry genetic information in the form of a control program for the biosynthesis of proteins [1]. Proteins and polypeptides have a tendency to fold spontaneously into their native conformation both in vivo and in vitro. However, these can be transformed from one conformation to another by varying pH, temperature, or surfactant solvent. Depending upon the size and type of interactions, the biopolymeric systems are capable of existing in a variety of secondary structures such as helical (α, 3-fold, and 4-fold), β-pleated sheet, planar zigzag, globular, bends, and random coil states [2]. Many of these structures are simultaneously present in a given chain. Generally, α, β, and random coils occur more frequently because of their inherent thermodynamic stability. Random coil generally occurs when a polypeptide contains adjacent bulky residues such as isoleucine or charged residue such as glutamic acid, aspartic acid. Repulsion between these groups causes the polypeptide to assume a random coil configuration. Bragg et al. [3] characterized another type of helical form 4_{13} termed as ω-helix, which is distorted α-helix. The ω-helix has a 4-fold screw axis in which there are four amino acid residues per helix turn with a residue translation of 1.3 Å and helix pitch of 5.2 Å. There are several other single-stranded intramolecularly hydrogen-bonded helices which have been proposed and found to exist, e.g., 2.2_7, 3_{10} (δ-helix), 5.1_{17} (γ-helix), 4.4_{16} (π-helix), 18_5 (α-helix), etc.

*Paper based on a presentation at POLYCHAR 16: World Forum on Advanced Materials, 17–21 February 2008, Lucknow, India. Other presentations are published in this issue, pp. 389–570.

‡Corresponding author: E-mail: poonam_tandon@hotmail.com

Several techniques have been used to characterize the conformation of polymeric systems. These include infrared (IR) absorption, Raman spectra, inelastic neutron scattering (INS), X-ray diffraction (XRD), nuclear magnetic resonance (NMR), circular dichroism (CD), and optical rotatory dispersion (ORD). These techniques are based on characteristic features such as IR absorption due to amide bands in a biopolymer and characteristic stretch modes in an industrial tactic polymer. However, none of these techniques reflects the characteristic dynamical feature within the first Brillouin zone of a vibrating polymer. INS, which is free from all kinds of constraints imposed by selection rules, reflects this dynamical feature through the density-of-states. However, it has its own problems in terms of resolution and sensitivity.

Vibrational spectroscopy plays an important role in the elucidation of polymeric structure, and it is intimately related to the symmetry of the polymers. In the present communication, we have tried to show how the dispersion profile of low-frequency modes reflects the symmetry of the polymer chain. This has been done in a variety of symmetry groups [4–16]. Strong supporting evidence of the spectral parameters (constants of IR and Raman) is obtained from quantum chemical [Hartree–Fock (HF), post-HF, and density functional theory (DFT)] [17–20] and molecular dynamical (MD) approaches. They have the additional advantage of including interchain interaction and anharmonic effects. The MD even enables modeling of disordered systems. The forgoing techniques have been widely used in a variety of systems [21–29].

An overall understanding of vibrational dynamics in a polymer involves calculation of the dispersion curves. These curves also provide knowledge of the degree of uninterrupted sequence lengths in an ordered conformation. The dynamics of a polymeric system is an order of magnitude more difficult than usual molecular systems because the phase relationship between the adjacent units has to be considered. This in turn necessitates recasting of kinetic and potential fields as a function of phase relationship. The dispersion curves also facilitate correlation of the microscopic behavior in a long-chain molecule with its macroscopic properties such as entropy, enthalpy, specific heat, etc.

THEORY

Molecular vibrations of finite molecules

In attempting to account for the observed IR and Raman spectra of real molecules, a certain simplified model is adopted and then the spectra that this model would exhibit are calculated. The model consists of particles endowed with mass and held together by electrical forces such as dipole–dipole interactions, covalent, etc. Particles represent the atoms and are treated as if all the mass were concentrated at a point. For a molecule having N atoms there are $3N$-6 vibrational degrees of freedom (or $3N$-5 if the molecule is linear). Using any set of generalized coordinates, the problem can be reduced to writing the secular equations to be solved to get eigen frequencies and eigen vectors. However, a brief description of Wilson's GF matrix method [30,31] is being given. It uses internal coordinates that are bond stretches, in-plane angle bending, torsions, and waggings. The internal coordinates are easiest and simplest and can best reflect the physical nature of molecular vibrations. They also permit the transferability of force constants from a group in one molecule to the corresponding group in another molecule in a similar environment. The small amplitude and harmonic nature of molecular vibrations provide a linear transformation between various displacement coordinates. The internal coordinates R are related to the Cartesian coordinate X in matrix notation as follows.

$$R = BX \tag{1}$$

where R is the internal coordinate and B is the transformation matrix and depends upon the geometry of the molecule. Then, the G-matrix or the inverse kinetic energy matrix is defined by the relation

$$G_{kl} = \sum_{i=1}^{3n} B_{ki} B_{li} / m_i \qquad (k,l = 1 \ldots\ldots\ldots\ldots, 3n-6) \tag{2}$$

where m_i is the mass of the i^{th} atom.

$$G = BM^{-1} B'$$

$$|G| = \begin{vmatrix} G_{11}G_{12} \ldots G_{1n} \\ G_{21}G_{22} \ldots G_{2n} \\ \ldots\ldots\ldots\ldots \\ G_{n1}G_{n2} \ldots G_{nn} \end{vmatrix}$$

The kinetic energy of vibration can be written in terms of the internal coordinates in the form

$$2T = \dot{R}' G^{-1} \dot{R} \tag{3}$$

where R' denotes the transpose of R.

The potential energy is given by the expression

$$2V = R'FR \tag{4}$$

where F is the potential energy matrix and its elements are linear function of the force constants f_k. In practice, it is computed through the basis matrix (z-matrix) where

$$F_{ij} = \sum_k z_{ijk} f_k$$

The coefficients z_{ijk} (z-matrix) are determined by the geometry of the molecule. The molecular vibrational problem is then represented by the matrix equation

$$GFL = \lambda L \tag{5}$$

where the eigen values λ's are related to the vibrational frequencies ν's by $\lambda = 4\pi^2 c^2 \nu^2$ and the normal coordinates Q are related to the internal coordinates R by

$$R = LQ \tag{6}$$

To obtain the vibrational frequencies, one has to solve the secular equation

$$|GF - \lambda I| = 0 \tag{7}$$

where I is the unit matrix.

In each normal mode of vibration, all the atoms in a molecule vibrate in phase with the same frequency ν_k at a particular instant. They may have different amplitudes. The extant of vibrational coupling between the various internal displacement coordinates, in a given normal mode Q_k is qualitatively described by the elements of the eigenvector L_k belonging to the eigenvalues λ_k.

Because of the different dimensions of L vectors for stretching and bending coordinates, it is preferable to use the potential energy distribution (PED) to characterize the energy distribution. The PED is the fractional part of potential energy of the normal mode vibration contributed by each force constant. If each $F_{ij}L_{ik}L_{jk}$ term is divided by the total sum of $F_{ij}L_{ik}L_{jk}$ terms for this vibration (which is equal to λ_k), then

$$\left(PE\right)_i^k = \frac{L_{ik}^2 F_{ii}}{\lambda_k} \tag{8}$$

where the L vectors have been defined previously. The PED is useful in making the assignment of various frequencies.

Symmetry considerations in finite molecules

In this section, the importance of the symmetry of the molecule and group-theoretical ideas is elucidated. For a molecule having M atoms, the dimensions of the secular equation are $(3M \times 3M)$, and it is quite cumbersome to solve the problem even for a molecule of moderate size. But in the case of the symmetric molecule, the secular equation can be factored into blocks of smaller dimensions by using internal symmetry coordinates [32]

$$S_m^{(\gamma)} = N\sum_O X_O^{(\gamma)} OR_m \tag{9}$$

where γ is the particular symmetry species, N is the normalization factor, O is the symmetry operation, $X_O^{(\gamma)}$ is the character of the γ species for O^{th} operation, and OR_m stands for the internal coordinate to which R_m is transformed by the operation O.

Applying group theory, the number of normal modes in a particular symmetry species (γ) is given as

$$n^{(\gamma)} = 1/H\sum_j g_j X_j^{(\gamma)*} X_j \tag{10}$$

Here, H is the order of the point group, g_j is the number of symmetry operations in the j^{th} class, $X_j^{(\gamma)}$ is the character of the γ species in the j^{th} class, and X_j is the character of the j^{th} symmetry transformation of the displacement coordinates.

The symmetry of the molecule can be exploited in solving the secular equation by transforming the kinetic and potential energy matrices in the space of symmetry coordinates. The dynamical matrices when transformed in the space of symmetry coordinates factor in blocks belongs to one of the symmetry species. The internal coordinates are related to the symmetry coordinates. In the matrix notation

$$S = UR \tag{11}$$

U is a transformation matrix obtained from the coefficients of symmetry coordinates and it is used to diagonalize into blocks, G and F matrices

$$G^B = U'GU \tag{12}$$

$$F^B = U'FU \tag{13}$$

U' is the transpose of U. So the modified secular equations becomes

$$|G^{(\gamma)} F^{(\gamma)} - \lambda I| = 0 \tag{14}$$

These can be solved completely independent of each other for individual symmetry species.

Molecular vibrations of polymer chains

The basic concepts discussed in the previous section can be applied to polymer chains but as the polymer molecule is of infinite length, the order of the matrices becomes infinite. In order to reduce the problem to one of workable dimensions, the screw symmetry of the polymer chain is exploited. The polymer chains are built up of chemical units or monomers arranged in a regularly repeating fashion. Higgs [33] was the first to point out the importance of the helical symmetry present in polymer molecules and utilize it in order to adapt the Wilson's GF matrix for polymeric systems. He considered in a fairly general manner the vibrations of a helical molecule and used group-theoretical ideas to classify the normal modes and derive the selection rules for Raman and IR spectra.

According to Higgs treatment, an infinite helical molecule is built of identical units linked together in such a way that each unit is transformed geometrically into the next by the operation $H(l, f)$. This operation is defined by a translation through a distance l along the axis plus a rotation through an angle f about the same axis. Thus, any group in the chain can be transformed into another group $\pm n$ units away by operating with H^n (n is any integer positive or negative). This operation transforms one unit into another and constitutes an infinite group that is simply isomorphic with the infinite cyclic group C_∞. Its irreducible representations are, therefore, all one-dimensional, and may be labeled $\Gamma(\theta)$ with parameter (θ) which runs through all values in the range $-\pi \leq \theta \leq +\pi$ the corresponding characters are given by

$$\chi(\theta, H^n) = \exp(in\theta) \tag{15}$$

Every normal mode of vibration of molecule must belong to one of these representations. This means that if in a normal mode a certain unit vibrates in some manner with an amplitude A, then the n^{th} unit further must vibrate in the same manner with an amplitude $A\exp(-in\theta)$. Each frequency ν_i of an isolated unit gives rise to a band of frequencies $\nu_i(\theta)$ in the helically linked molecule, where θ is the phase difference between adjacent units. It can be shown that corresponding to each frequency $\nu_i(\theta)$, there lies a frequency $\nu_i(-\theta)$, which is equal to $\nu_i(\theta)$. Thus, with the exception of $\nu_i(0)$ and $\theta_i(\pi)$, the frequencies are degenerate in pairs belonging to $\Gamma(\theta)$ where $(0 \leq \theta \leq +\pi)$. Therefore, the corresponding complex normal modes can be combined to form two real ones in which the amplitudes vary as (A cos $n\theta$) and (A sin $n\theta$).

Coming to the solution of the vibrational secular equation, let R_i^n denote the i^{th} internal displacement coordinate belonging to the n^{th} chemical unit. Then the potential interaction and the kinetic coupling between the i^{th} internal coordinate and the n^{th} unit and the k^{th} internal coordinate of the n^{th} unit are given by the matrix element $F_{ik}^{nn'}$ and $G_{ik}^{nn'}$. Now the periodicity of the chain requires that these matrix elements depend on n and n' only through their differences, that is,

$$F_{ik}^{nn'} = F_{ik}^{S} \tag{16}$$

$$G_{ik}^{nn'} = G_{ik}^{S} \tag{17}$$

where $S = (n-n')$. In view of this, a particular portion of the infinite G matrix can be written in terms of R's as coordinates,

	$\cdots$	$\bar{R}^{n-3}$	$\bar{R}^{n-2}$	$\bar{R}^{n-1}$	$\bar{R}^{n}$	$\bar{R}^{n+1}$	$\bar{R}^{n+2}$	$\bar{R}^{n+3}$	$\cdots$
$\vdots$									
$\bar{R}^{n-3}$		G_A	G'_B	G'_C	G'_D				
$\bar{R}^{n-2}$		G_B	G_A	G'_B	G'_C	G'_D			
$\bar{R}^{n-1}$		G_C	G_B	G_A	G'_B	G'_C	G'_D		
$\bar{R}^{n}$		G_D	G_C	G_B	G_A	G'_B	G'_C	G'_D	
$\bar{R}^{n+1}$			G_D	G_C	G_B	G_A	G'_B	G'_C	
$\bar{R}^{n+2}$				G_D	G_C	G_B	G_A	G'_B	
$\bar{R}^{n+3}$					G_D	G_C	G_B	G_A	
$\vdots$									

where $\bar{R}^n$ is the column vector of internal coordinates of the n^{th} chemical units. G_A', G_B',... denote the transposition of G_A, G_B,… The F matrix also has an analogous structure.

Higgs showed that the G and F matrices that are of infinite order can be factored into sets of matrices $G(\delta)$ and $F(\delta)$ which are of finite order, corresponding to the phase difference δ between the vibration of adjacent units in the chain. The order of $G(\delta)$ and of $F(\delta)$ is equal to N (the number of internal coordinates in a chemical repeat unit). A Fourier transform on the system of internal displacement coordinate is defined, in order to give a set of internal symmetry coordinates

$$S(\delta) = \sum_{n=-\infty}^{\infty} R^n \exp(in\delta) \tag{18}$$

The elements of the $G(\delta)$ and $F(\delta)$ matrices are then

$$G_{ik}(\delta) = \sum_{n=-\infty}^{\infty} G_{ik}^s \exp(in\delta) \tag{19}$$

$$F_{ik}(\delta) = \sum_{n=-\infty}^{\infty} F_{ik}^s \exp(in\delta) \tag{20}$$

The secular equation of an infinite order can then be reduced to a set of n^{th}-order equations

$$|G(\delta)F(\delta) - \lambda(\delta)I| = 0 \tag{21}$$

where the vibrational frequencies are given by $\lambda(\delta) = 4\pi^2c^2\nu^2(\delta)$ [where $\nu(\delta)$ is expressed in cm^{-1}] and $-\pi \le \delta \le +\pi$.

Symmetry properties and selection rules

The vibrational frequencies calculated by eq. 21 are infinite in number but only a few of them are optically active in polymers. Selection rules for such molecules were first worked out by Higgs, in terms of the phase difference δ and the angle ϕ. It is well known that the only frequencies which appear as allowed fundamentals in IR absorption are those belonging to representation $\Gamma(\theta)$, and it is essential that these are contained in the representations $\Gamma(\bar{M})$ which has, as its basis, the components of the total molecular electric dipole moment $\bar{M}$. It turns out that IR absorption arises either from the a vibrations with phase difference $\delta = 0$ (the transition moment being parallel to the helix axis) or from the $E(\phi)$ vibration with $\delta = \phi$ (the transition moment being perpendicular to the axis).

In order to derive the Raman selection rules, one has to consider the total molecular electric polarizability. It can be shown that Raman absorption arises from the vibrations with phase difference $\delta = 0, \pm\phi, \pm 2\phi$.

Use of group-theoretical ideas

At this point, the importance of group-theoretical ideas in an understanding of polymer spectra needs to be described. This importance arises because the symmetry of a helical polymer can be described by a one-dimensional space-group. As mentioned earlier, only the normal modes in which all the unit cells vibrate in the same phase are active in the IR and Raman scattering [34]. Thus, it is sufficient spectroscopically to study only the factor group of the one-dimensional space group, which has the translational subgroup as the unit element. Let us consider an infinite helical molecule in which the one-dimensional crystallographic repeat unit contains n chemical units and m turns (each chemical repeat unit contains p atoms). In such a molecule, the basic symmetry operation is defined by a rotation of $2m\pi/n$ about the axis of the helix followed by a translation along the axis of $1/n$ of the unit cell length. The factor group in question may be denoted by $C_{2m\pi/n}$, which is isomorphic with the point group C_n. An analysis of the factor group of the polymer is useful in predicting the number of normal modes, their symmetry properties, and IR and Raman activity (Table 1) [35]. Coupled with dichroic studies on polymer spectra, an analysis of the symmetry group of the polymer can help in the analysis and interpretation of the spectra, even in the absence of complete normal vibration calculation. Liang and coworkers [36–41] have used these group-theoretical ideas to interpret the spectra of a large number of high polymers such as polyethylene, polytetrafluorethylene, polystyrene, polyvinyl chloride, etc. The work has been reviewed by Krimm [42].

Table 1 Character table, numbers of normal modes, and selection rules (A: active, F: forbidden) for the helical polymer molecule under the group $C_{2m\pi/n}$ [35].

n = odd

	E	C^1	C^2	…	C^{n-1}	N	IR	Raman
A	1	1	1	…	1	$3p(T_\pi,R_\pi)$	A	A
E_1	1	ε	ε^2	…	ε^{n-1}	$3p(T_\sigma)$	A	A
	1	ε^{-1}	ε^{-2}	…	$\varepsilon^{-(n-1)}$	$3p(T_\sigma)$	A	A
E_2	1	ε^2	ε^4	…	$\varepsilon^{2(n-1)}$	$3p$	F	A
	1	ε^{-2}	ε^{-4}	…	$\varepsilon^{-2(n-1)}$	$3p$	F	A
E_3	1	ε^3	ε^6	…	$\varepsilon^{3(n-1)}$	$3p$	F	F
	1	ε^{-3}	ε^{-6}	…	$\varepsilon^{-3(n-1)}$	$3p$	F	F
.	.	.	.	…	.	.	.	.
.	.	.	.	…	.	.	.	.
$E_{(n-1)/2}$	1	$\varepsilon^{(n-1)/2}$	$\varepsilon^{[(n-1)/2]2}$	…	$\varepsilon^{[(n-1)/2](n-1)}$	$3p$	F	F
	1	$\varepsilon^{-(n-1)/2}$	$\varepsilon^{-[(n-1)/2]2}$	…	$\varepsilon^{-[(n-1)/2](n-1)}$	$3p$	F	F

(*continues on next page*)

Table 1 (*Continued*).

n = even

	E	C^1	C^2	…	C^{n-1}	N	IR	Raman
A	1	1	1	…	1	$3p(T_\pi,R_\pi)$	A	A
B	1	–1	1		–1	$3p$	F	A
E_1	1	ε	ε^2	…	ε^{n-1}	$3p(T_\sigma)$	A	A
	1	ε^{-1}	ε^{-2}	…	$\varepsilon^{-(n-1)}$	$3p(T_\sigma)$	A	A
E_2	1	ε^2	ε^4	…	$\varepsilon^{2(n-1)}$	$3p$	F	A
	1	ε^{-2}	ε^{-4}	…	$\varepsilon^{-2(n-1)}$	$3p$	F	A
E_3	1	ε^3	ε^6	…	$\varepsilon^{3(n-1)}$	$3p$	F	F
	1	ε^{-3}	ε^{-6}	…	$\varepsilon^{-3(n-1)}$	$3p$	F	F
.	.	.	.	…	.	.	.	.
.	.	.	.	…	.	.	.	.
$E_{[(n/2-1)]}$	1	$\varepsilon^{[(n/2)-1]}$	$\varepsilon^{[(n/2)-1]2}$	…	$\varepsilon^{[(n/2)-1](n-1)}$	$3p$	F	F
	1	$\varepsilon^{-[(n/2)-1]}$	$\varepsilon^{-[(n/2)-1]2}$	…	$\varepsilon^{-[(n/2)-1](n-1)}$	$3p$	F	F

where $\varepsilon = \exp[i(2m\pi/n)]$

Calculation on actual polymers

For a polymer chain, the normal vibrational treatment can be carried out in terms of the internal displacement coordinates. In the present study, the method used in the vibrational analysis of polymers is the same as that described by Piseri and Zerbi [43]. Let us consider the ideal polymer chain which can be geometrically constructed by applying a screw-symmetry operation to the starting chemical repeat unit. In the quadratic approximation, the vibrational potential energy of such systems, $V = V(R_i^n)$, where R_i^n are the i^{th} internal coordinates of the n^{th} residue, can be expressed in Taylor's series about the equilibrium configuration and the expansion truncated to second order when the harmonic approximation is adopted

$$V = V_o + \sum_{n,i} \left(F\right)_i^n R_i^n + \frac{1}{2} \sum_{n,n'} \sum_{i,k} \left(F\right)_{ik}^{nn'} R_i^n R_k^{n'} \tag{22}$$

where $\left(F\right)_i^n = \left[\dfrac{\partial V}{\partial \left(R\right)_i^n}\right]_{eq.}$ and $\left(F\right)_{ik}^{n,n'} = \left[\dfrac{\partial^2 V}{\partial R_i^n \partial R_k^{n'}}\right]_{eq.}$

Since at equilibrium the system possesses a minimum potential energy, $(F)_i^n$ is equal to zero. After a suitable shifting of axes, the potential energy in harmonic approximation can be written as

$$2V = \sum_{n,n',i,k} F_{ik}^{nn'} R_i^n R_k^{n'} \tag{23}$$

Making use of the periodicity of the chain, it follows that

$$2V = \sum_{n,i,k} F_{ik}^0 R_i^n R_k^n + \sum_{n,s,i,k} \left(F_{ik}^s R_i^n R_k^{n+s} + F_{ki}^s R_i^n R_k^{n-s}\right) \tag{24}$$

The kinetic energy of the infinite chain can be written in an analogous way in terms of the momenta P^n conjugate to the coordinates R_i^n and the kinetic energy matrix G.

$$2T = \sum_{n,i,k} G_{ik}^{0} P_i^n P_k^n + \sum_{n,s,i,k} \left(G_{ik}^{s} P_i^n P_k^{n+s} + G_{ki}^{s} P_i^n P_k^{n-s} \right) \tag{25}$$

Hamiltonian's equation of motion can be written using eqs. 24 and 25, thus leading to a system of an infinite number of second-order differential equations in the R_i^{n+s} whose solution can be assumed to be planar wave

$$R_i^{n+s} = A_i \exp\left[-i(\lambda^{1/2}t + s\delta)\right] \tag{26}$$

Here, δ is phase shift between two equivalent internal displacement coordinates in adjacent units. Substitution of eq. 26 into the system of differential equations yields a system of $3p$ simultaneous homogeneous linear equations (p is the number of atoms in a chemical repeat unit) in the unknowns A_i, whose nontrivial solutions are given by the equation

$$|G(\delta)F(\delta) - \lambda(\delta)I| = 0 \tag{27}$$

where $\lambda(\delta) = 4\pi^2 c^2 \nu^2(\delta)$ and

$$G(\delta) = G^0 + \sum_s \left[G^s \exp(is\delta) + G^{s'} \exp(-is\delta) \right] \tag{28A}$$

$$F(\delta) = F^0 + \sum_s \left[F^s \exp(is\delta) + F^{s'} \exp(-is\delta) \right] \tag{28B}$$

Equations 28A and 28B coincide with those first given by Higgs eqs. 19 and 20 through a Fourier transform on the system of internal displacement coordinates. A calculation of $\nu(\delta)$ as a function of δ gives the dispersion curves. This function is periodic with a period equal to 2π, i.e., $n(\delta + 2\pi)$. Further, $\nu(-\delta) = \nu(\delta)$ so that one can limit a study of the function to the range $0 \le \delta \le \pi$, which corresponds to half of the first Brillouin zone (reduced zone scheme). Optically active frequencies correspond to values of $\delta = 0, \phi, 2\phi$.

For any given phase difference δ (other than *0* or π), the $G(\delta)$ and $F(\delta)$ matrices are complex. A number of difficulties arise in handling complex numbers. In order to avoid these difficulties, certain methods have been proposed to convert matrices into equivalent real matrices. This can be done by constructing suitable linear combinations of coordinates, as mentioned in eq. 9. It can be shown that any complex matrix can be set to its real equivalent through a suitable similarity transformation. If C is a complex matrix with a real part X and an imaginary part Y, it can be written as

$$C = \begin{bmatrix} X + iY & 0 \\ 0 & X - iY \end{bmatrix} \tag{29}$$

It can be transformed into its real equivalent R by matrix

$$R = PCP^{-1} = \begin{bmatrix} X & -Y \\ Y & X \end{bmatrix} \tag{30}$$

$$\text{where } P = \frac{1}{\sqrt{2}} \begin{bmatrix} I & I \\ -iI & iI \end{bmatrix} \tag{31}$$

And I is the identity matrix of order $3p$.

In the present case, we can write $G(\delta) = G^R(\delta) + iG^I(\delta)$ and $F(\delta) = F^R(\delta) + iF^I(\delta)$, where $G^R(\delta)$, $F^R(\delta)$, $G^I(\delta)$, $F^I(\delta)$ are the real and imaginary parts of $G(\delta)$ and $F(\delta)$. The product $H(\delta) = G(\delta)\,F(\delta)$ becomes

$$\begin{vmatrix} G^R(\delta) & -G^I(\delta) \\ G^I(\delta) & G^R(\delta) \end{vmatrix} * \begin{vmatrix} F^R(\delta) & -F^I(\delta) \\ F^I(\delta) & F^R(\delta) \end{vmatrix} = \begin{vmatrix} H^R(\delta) & -H^I(\delta) \\ H^I(\delta) & H^R(\delta) \end{vmatrix} \tag{32}$$

where $H^R(\delta) = G^R(\delta)F^R(\delta) - G^I(\delta)F^I(\delta)$ and

$$H^I(\delta) = G^R(\delta)F^I(\delta) - G^I(\delta)F^R(\delta) \tag{33}$$

The matrix $H(\delta)$ now has dimensions $2N \times 2N$. The eigen values, however, occur in pairs of equal values. The difficulty of dealing with complex number is thus avoided.

The polarization vectors, which give the components of the cartesian displacements of the atoms in the various normal modes, are an important result of normal coordinate calculations. For the mode $\nu(\delta)$ the polarization vectors are defined by

$$q(\delta) = B^{-1}(\delta)L(\delta) \tag{34}$$

where the $L(\delta)$ vectors are defined as in eq. 6.

Force field

In the present work, we have used the Urey–Bradley force field [44] as it is more comprehensive then the valence force field. The Urey–Bradley takes into account both bonded and nonbonded interactions as well as internal tensions. Potential energy for this force field can be written as

$$\begin{aligned} V = & \sum_{m,j,k} \left\{ K'_{j,k} r^{(m)}_{j,k} \left(\Delta r^{(m)}_{j,k} \right) + K_{j,k} \left(\Delta r^{(m)}_{j,k} \right)^2 / 2 \right\} + \\ & \sum_{m,i,j,k} \left\{ H'_{i,j,k} r^{(m)}_{i,j} r^{(m)}_{j,k} \left(\Delta \alpha^{(m)}_{i,j,k} \right) + H_{i,j,k} r^{(m)}_{j,k} \left(\Delta \alpha^{(m)}_{i,j,k} \right)^2 / 2 \right\} + \\ & \sum_{m,i,j,k} \left\{ F'_{i,k} q^{(m)}_{i,k} \left(\Delta q^{(m)}_{i,k} \right) + F_{i,k} \left(\Delta q^{(m)}_{i,k} \right)^2 / 2 \right\} + \sum_j K^{\tau}_j \left(\Delta \tau_j \right)^2 + \sum_j K^{\omega}_j \left(\Delta \omega_j \right)^2 \end{aligned} \tag{35}$$

where $\Delta r^{(m)}_{jk}$, $\Delta \alpha^{(m)}_{ijk}$, $\Delta \tau^{(m)}_j$ and $\Delta \omega^{(m)}_i$ are the internal coordinates corresponding to bond stretch, angle bend, torsion, and out-of-plane wag, respectively. The subscripts on the first three internal coordinates label the atoms involved, and the superscript m labels the chemical repeat unit. Nonbonded interactions involve attraction and repulsion of atoms due to the overlap of their electron shells. These effects are usually expressed by the 6-exp or 6-12 type potentials. The tension terms are assumed to be all zero.

Recently, spectroscopically effective molecular mechanics model have been used for inter- and intramolecular interactions consisting of charges, atomic dipoles, and van der Waals (nonbonded) interactions [45].

Theory of interpretation of spectra of oligomers

One of the most important uses of the dispersion curves is to expound the spectra of short-chain molecules or oligomers that have the same structure as the polymeric form. The IR spectra of macromolecules containing a finite chain of identical structural units as characterized by a series of absorption bands. It can be shown that the normal modes responsible for component absorption can be specified by an appropriate phase difference. They are denoted by k values related to the phase difference δ along the chain between adjacent residue units and are given by

$$\delta = (k\pi/n) \qquad (k = 0,1,2.....,n-1)$$

where n is the number of repeat units in the chain and k is an integer that represents the number of loops in a stationary wave representing the chain vibrations. The above equation holds good for finite chain having free ends.

Density-of-states and heat capacity

Another use of dispersion curves is that the microscopic behavior of a crystal can be correlated with its macroscopic properties such as specific heat. For a one-dimensional system, the density-of-states function or the frequency distribution function expresses the way energy is distributed among the various branches of normal modes in the crystal. This can be calculated from the relation

$$g(v) = \sum_j \left(\delta v_j / \partial\delta\right)^{-1}\Big|_{v_j(\delta)=v} \tag{36}$$

with $\int g(v_j)d\ v_j = 1$

The sum is over all branches j. If we consider a solid as an assembly of harmonic oscillators, the frequency distribution $g(v)$ is equivalent to a partition function. This can be used to compute thermodynamic quantities such as free energy, entropy, specific heat, and enthalpy. The heat capacity, which is an important thermodynamic parameter, can be calculated using the Debye relation. For example, the heat capacity can give information about the proportion of a protein, which is in α-helical and β-sheet structure and is necessary in evaluating the basic thermodynamics of the enzyme reaction [46]. The Debye relation is given by

$$C_v = \sum_j g\left(v_j\right) kN_A \left(hv_j / kT\right)^2 \frac{\exp\left(hv_j / kT\right)}{\left[\exp\left(hv_j / kT\right) - 1\right]^2} \tag{37}$$

The constant volume heat capacity C_v, given by eq. 43, is converted into constant pressure heat capacity C_p using the Nernst–Lindemann approximation [47]

$$C_p - C_v = 3RA_0 \left(C_p^2 T / C_v T_m^0\right) \tag{38}$$

where A_0 is a constant often of a universal nature and T_m^0 is the equilibrium melting temperature [48].

Quantum chemical methods

Application of quantum chemical techniques to real chemical systems represents the essence of computational chemistry. These techniques such as molecular orbital (MO) theory [49] and DFT [50–58] etc., are used to study molecular structure and conformational isomerism as well as molecular spectra such as vibrational and electronic. Quantum chemical methods may be broadly classified as semi-empirical and ab initio.

The semi-empirical methods, where the values of several integrals are obtained with the help of experimental parameters, are usually less accurate than the ab initio methods in the determination of molecular structure and thermal energy, though in certain cases of a series of related molecules, they can provide results in remarkable agreement with the experimental findings. However, in spectroscopic studies, which involve energy differences between various states, fairly reliable results have been obtained by both the ab initio and semi-empirical MO methods.

Various variants of semi-empirical all valence electron methods such as complete neglect of differential overlap (CNDO), intermediate neglect of differential overlap (INDO), modified intermediate neglect of differential overlap (MINDO), modified neglect of differential overlap (MNDO), etc. and the HF and post-HF ab initio methods have been used for conformational analysis of organic molecules.

Ab initio methods, unlike semi-empirical methods, use no experimental parameters in their computation. Instead, their computations are based solely on the laws of quantum mechanics. There are various theories underlying ab initio methods like closed- and open-shell HF theory and DFT. HF theory provides an inadequate treatment of the correlation between the motions of the electrons within a molecular system. The motion of electrons of opposite spin remains uncorrelated in this scheme. The techniques are widely used to incorporate the effect of electron correlation (i) configuration interaction and (ii) Moller–Plesset perturbation theory.

The first method is variational but not size-consistent, whereas the second is size-consistent but not variational. Variational implies that the calculated electronic energy should correspond to an upper bound to the energy that would result from the exact solution of the Schrödinger equation. Size consistency means that the method must give additive results when applied to an assembly of isolated molecules.

RESULTS AND DISCUSSION

Polypeptides

Polymeric systems in general and biopolymers in particular are capable of existing in a variety of conformations. Almost all their properties are dictated by the type of conformation taken up by the biomolecules. The spectroscopic approach has proved a very powerful diagnostic tool in characterizing their conformation. However, the problem is an order of magnitude more complex than in simple solids, mainly because of the absence of simple symmetry and presence of large contents in unit cell. For example, polyalanine ($R=CH_3$), which is a very simple polypeptide, has in the one-dimensional unit cell 18 residues and 5 turns. Each residue has 10 atoms. The problem thus has enormous dimensions. Further, the coupling of normal vibrations of successive repeat units necessitates evaluation of the dispersion of the normal modes in the first Brillouin zone. This has been done for the whole set of normal modes in α, β, ω, and 3-fold helices, which are the conformations generally taken up by most of the polypeptides. Apart from the characteristic amide bands, it is observed that the profile of the low-frequency modes including the acoustic modes reflects the skeletal conformation beautifully well. This provides a good handle for conformation classification on the basis of the dispersion profile [4]. The results are presented for α-helical [poly(L-valine) (PLV), poly(L-leucine) (PLL), poly(L-glutamic acid) (PLG), poly(β-benzyl-L-aspartate) (PBLA)], β-sheet [poly(L-serine) (PLS), PLV], ω-helical [PBLA, poly-N^{ε}(*p*-bromobenzoyl-L-ornithine) (PBRBO)], and 3-fold [polyglycine II (PG II), poly-(L-hydroxyproline) (PLHP), poly-L-proline II (PLP II)] polypeptides [5–16].

Conformation of a polypeptide, protein, or nucleic acid to a very large extent dictates its physicochemical, thermodynamical, hydrodynamical, and biological behavior. It is determined by both the covalent as well as noncovalent interactions. The latter part includes hydrophobic, van der Waals, electrostatic, and hydrogen bond interactions. The nonbonded interactions can be visualized at two levels, namely, short- and long-range interactions. The short range comprises the backbone and side chain, whereas the long range arises out of side chain–side chain interactions. Various physicochemical techniques have been used as diagnostic tools to characterize the conformations, viz., NMR, IR, CD, XRD, etc. Most of the polypeptides go into four main types of structures, i.e., Pauling's α-helix, pleated-sheet β structure, 4-fold ω-helix, and 3-fold collagen-type helix. The structures are shown in Figs. 1b, 2b, 3b, and 4b, respectively. The low-frequency acoustic and optical modes for these chain structures are shown alongside. Spectroscopically speaking, the amide modes that are used for identification of various conformations are shown in Tables 2 and 3.

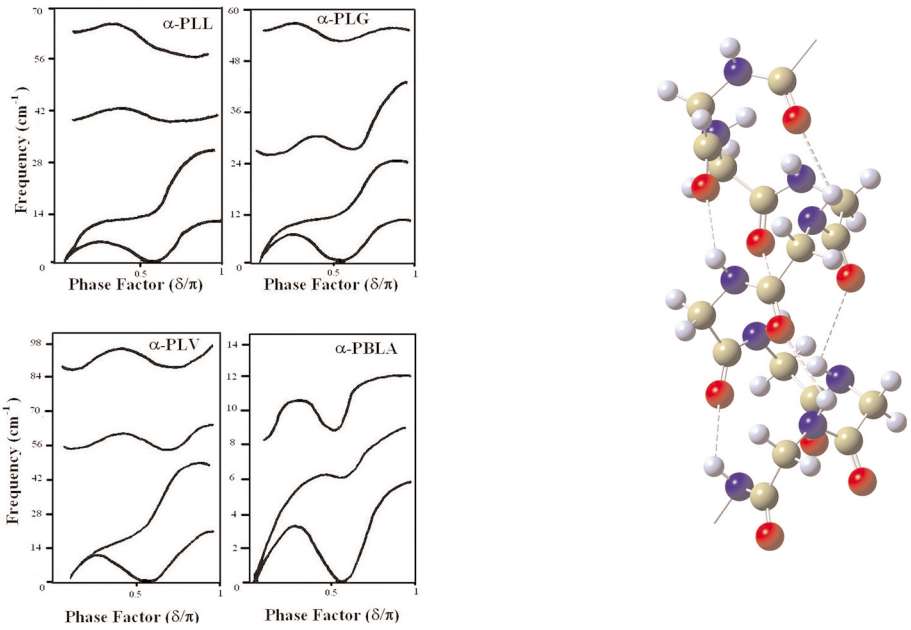

Fig. 1 (a) Low-frequency dispersion curves of α-helical polypeptides. PLL: poly(L-leucine) [5]; PLG: poly(L-glutamic acid) [6]; PLV: poly(L-valine) [7]; PBLA: poly(β-benzyl-L aspartate) [8]. (b) α-helix.

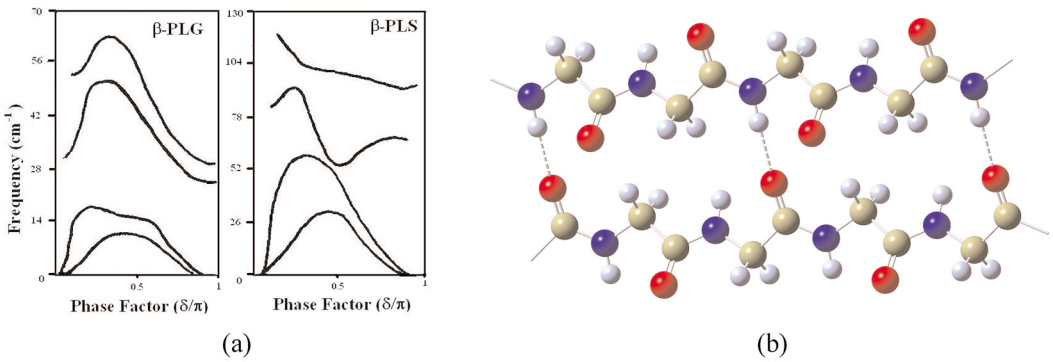

Fig. 2 (a) Low-frequency dispersion curves of β-sheet polypeptides. PLG: poly(L-glutamic acid) [9]; PLS: poly(L-serine) [10]. (b) β-sheet (polyglycine-I).

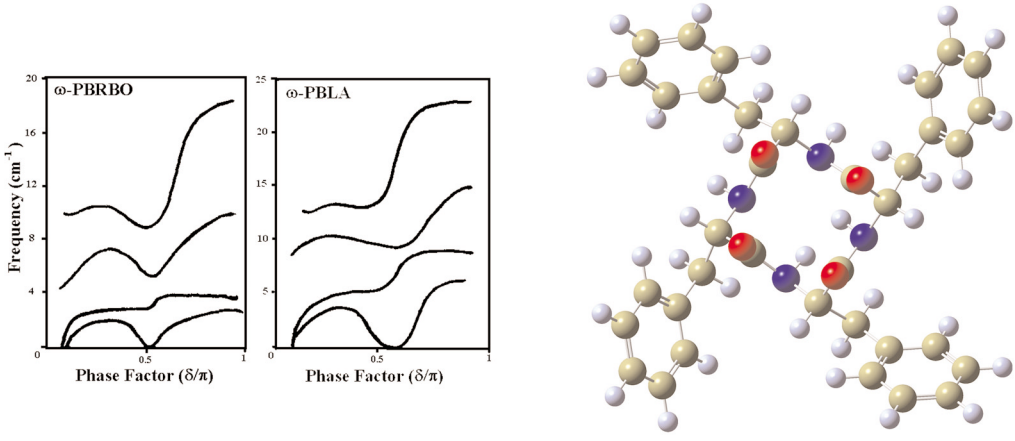

(a) (b)

Fig. 3 (a) Low-frequency dispersion curves of ω-helical polypeptides. PBRBO: poly-N^{ϵ}(*p*-bromobenzoyl-L-ornithine) [11]; PBLA: poly(β-benzyl-L-aspartate). (b) ω-helix (projection perpendicular to helix axis).

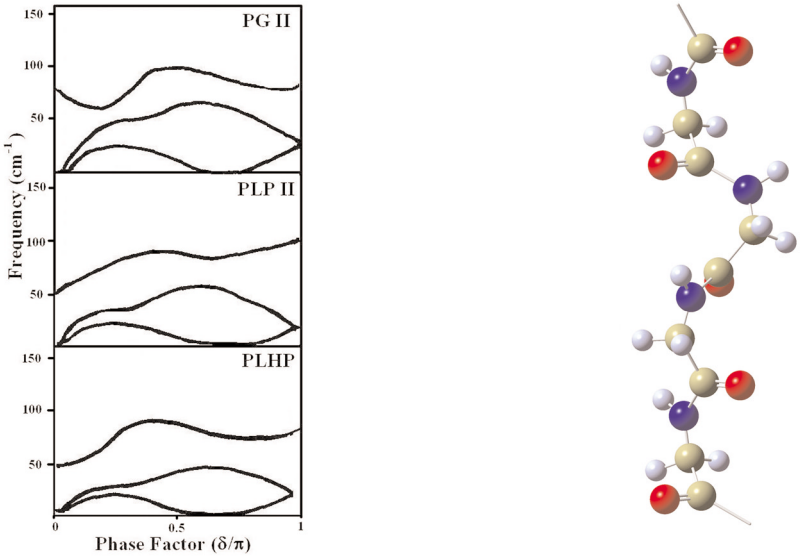

(a) (b)

Fig. 4 (a) (i) Low-frequency dispersion curves of 3-fold polypeptides. PG II: polyglycine II; PLP II: poly(L-proline) II; PLHP: poly(L-hydroxyproline) [4]. (b) 3-fold helix (polyglycine-II).

Table 2 Comparison of amide modes of polypeptides having β-sheet conformation.

Amide	Poly(L-serine)		Polyglycine I		Poly(L-alanine)		Poly(L-glutamic acid)		Poly(L-valine)	
	$\delta = 0$	$\delta = \pi$	$\delta = 0$	$\delta = \pi$	$\delta = 0$	$\delta = \pi$	$\delta = 0$	$\delta = \pi$	$\delta = 0$	$\delta = \pi$
A	3318	3318	3300	3300	3283	3283	3230	3230	3290	3290
I	1637	1628	1690	1630	1695	1634	1624	1624	1638	1638
II	1532	1537	1514	1524	1524	1524	1560	1560	1545	1545
III	1249	1270	1240	1220	1224	1241	1259	1241	1228	1228
IV	533	773	628	773	594	657	549	258	548	684
V	713	685	699	700	622	705	705	705	715	715
VI	533	647	618	600	594	657	653	643	615	626

All frequencies are in cm^{-1}.

Table 3 Comparison of amide modes of α-helical polypeptides.

Amide	Poly (L-glutamic acid)		Poly(L-valine)		Poly(L-alanine)		Poly(L-leucine)		Poly (β-benzyl-L-aspartate)	
	$\delta = 0$	$\delta = 5\pi/9$	$\delta = 0$	$\delta = 5\pi/9$	$\delta = 0$	$\delta = 5\pi/9$	$\delta = 0$	$\delta = 5\pi/9$	$\delta = 0$	$\delta = 5\pi/9$
A	3301	3301	3293	3293	3293	3293	3313	3313	3300	3300
I	1652	1652	1655	1650	1659	1659	1657	1657	1666	1666
II	1510	1550	1535	1520	1515	1540	1546	1578	1556	1556
III	1283	1283	1246	1253	1270	1274	1299	1318	1298	1298
IV	–	656	578	550	525	440	587	633	664	664
V	596	618	622	612	595	610	587	617	561	616
VI	670	–	691	691	685	656	656	533	669	595
VII	240	105	125	130	238	190	227	171	–	–

All frequencies are in cm^{-1}.

During the course of our studies on the normal vibrations and their dispersion in a variety of systems, it is observed that the profiles of the low-frequency dispersion curves (acoustic modes and lowest optical mode) bear a great deal of resemblance among biopolymeric systems that belong to the same symmetry. Since this coupling spreads over the entire backbone, these coupled torsional and angle band deformation modes reflect the conformation of the chain. They are highly cooperative modes. The role of the side chains or the groups linked with the C_α atom results in affecting the PED and frequency of the mode at the zone center or at the critical points which occur at or around the same value of the wave vector in all systems belonging to the same symmetry, although the frequency value is different. It is not very surprising because they arise due to coupled torsional modes or in-plane skeletal angle bends. The similarity of the dispersion curve profile of the acoustic modes and low-frequency optical modes as shown for α-helix (Fig. 1a), β-sheet (Fig. 2a), ω-helix (Fig. 3a), 3-fold (Fig. 4a) is indeed very remarkable. Minor deviations could arise due to side chain–side chain interaction, particularly in helical configurations when they tend to be closer. The short-range interactions certainly play an important role, but they are eventually stabilized by long-range interactions.

For the β form there is slight deviation in optical modes, which is mainly due to difference in the strength of intra- and interchain interactions. The very fact that several polypeptide chains having different side chains or side groups prefer to go into α-helix, in a way, supports the contention that their low-frequency dispersion curves have resembling profiles. The same argument can be extended to the case of ω-helices in systems as varying as PBLA and PBRBO). For the last two cases, dispersion curves are shown in Fig. 3a. Our preliminary work on bare helices (chains divested of side groups) for these

symmetries also appears to be broadly in support of it. The low-frequency dispersion curve profiles are thus characteristic of their conformation.

Interpretation of spectra of oligomers from dispersion curves

In the absence of INS data, one of the easiest ways to test the meandering part of the dispersion curves is to look at the spectra of various oligomers. As discussed earlier, the spectra of oligomers are related to the dispersion profile of the polymer modes through the phase relationship given by the above expression and provided that both oligo and polymers are conformationally connected. The Raman scattering data on oligomers of valine up to the hexamer as reported by Fasman et al. [59] have been used. The observed modes are assigned at appropriate phase values on the corresponding branch of the dispersion curve from all the possible k values and are plotted in Fig. 5a along with the dispersion curve

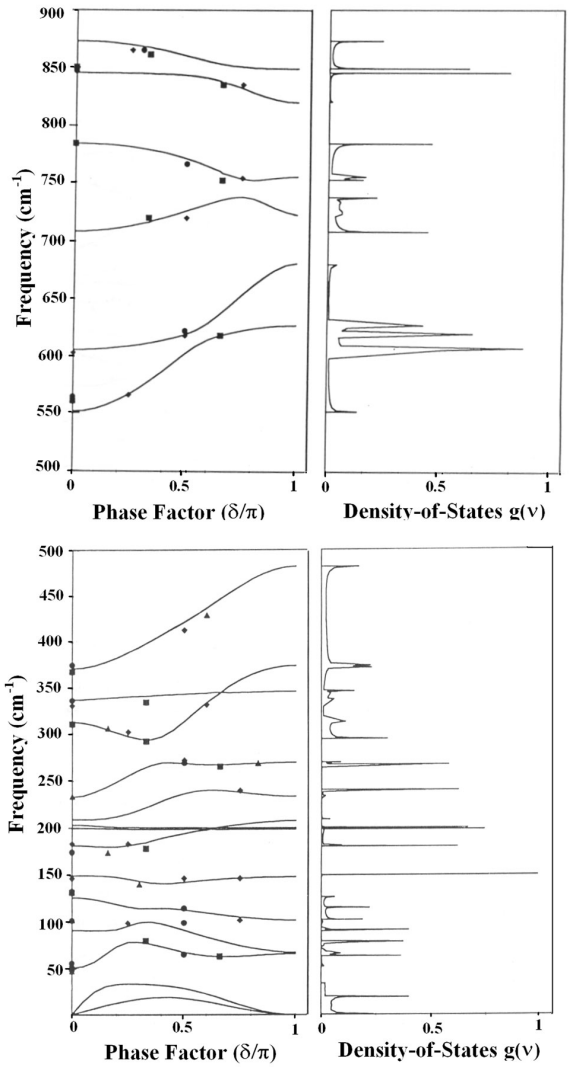

Fig. 5 (a) Dispersion curves of β PLV [13]. (b) Density-of-states of β PLV [13].

of $(Val)_n$ [13]. For example, for a trimer the phase values are 0, π/3, 2π/3. Considering the dispersion curve for a torsional mode having $\nu = 51$ cm^{-1} ($\delta = 0$), these phase values fall at frequencies 50, 78, and 62 cm^{-1}, respectively, and correspond to observed frequencies at 50, 80, and 63 cm^{-1}. It may be added that not all frequencies corresponding to various oligomers and different k values have been observed. The assignments thus made correspond to definite phase values. Table 4 gives a comparison of some important modes in various oligomers. A good agreement of observed frequencies for oligovalines on the corresponding dispersion curves for allowed phase values shows that the oligomers of valine up to hexamer have a structure closer to the extended β-form. In the case of di-valine there are significant deviations: these could be due to the end-group interactions arising from the out-of-plane conformation of the COO^- group with respect to the plane of the atoms in the skeleton (N–C_α–C–N). The interactions decay rapidly as the chain length increases [59].

Table 4 Comparison of spectra of oligovalines with its predictive values from the dispersion curves.

Mode	$n = 2$	$n = 3$	$n = 4$	$n = 6$	β-PLV
Amide I	1622(1630)	1655(1637)	1634(1631)	–	1629
	1660	1668	1663	1663	
Amide II	1551(1531)	1560(1537)	1565(1537)	1565(1537)	1537
Amide III	1254(1256)	1253(1255)	1238(1253)	1228(1250)	1256
Amide IV	564(551)	560(551)	566(566)	–	551
Amide V	744(726)	720(715)	720(713)	–	708
Amide VI	622(619)	618(606)	618(609)	–	606
Amide VII	133(127)	132(127)	102(106)	–	126
ν(N–C_α) + ν(C_α–C)	1072(1066)	1070(1076)	1087(1080)	1092(1086)	1086
	1031(1034)	1032(1037)	–	–	1038
Methyl rock	1003(1006)	1005(1006)	1014(1006)	1017(1005)	1006
ν(C_α–C) + ν(C=O)	936(934)	944(941)	954(944)	954(947)	949
	847(843)	850(845)	835(832)	844(845)	845
ω(N–H) + ω(C=O)	766(771)	784(784)	754(753)	756(760)	784
Main-chain deformation	269(269)	265(263)	272(268)	269(267)	270
Side-chain deformation	–	–	147(146)	141(143)	150
	375(371)	368(371)	400(398)	403(398)	371

All frequencies are in cm^{-1}, and the figures in parentheses are the predicted values from the dispersion curves of β-PLV for n = 2, 3, 4, and 6.

Biodegradable polymers

In the last century, plastic products have gained universal use but recently societal, environmental, and regulatory drivers are pushing industry to design and engineer products from "cradle to grave". Plastics are resistant to biological degradation because microorganisms do not have an enzyme capable of degrading and utilizing most man-made polymers. In the continuing search for suitable polymers to solve the environmental concerns, biodegradable polymers are useful options. The term "biodegradable polymers" refers to a polymer or plastic material that undergoes enzymatic degradation in the physiological or microbial environment. It is the processes in which a product is capable of being broken down into innocuous subproducts like CO_2 and water, by the action of living organisms/microorganisms such as bacteria, fungi, and algae.

Polyglycolic acid (PGA) $[–CH_2–COO–]_n$ and poly(ε-caprolactone) (PCL) $[–(CH_2)_5–COO–]_n$ are bioresorbable synthetic polymers that are used to make biomedical and pharmaceutical devices (Fig. 6). Both have a planar zigzag conformation. On comparing the dispersion curves of PGA and PCL, the lower modes are dispersive, and an interesting feature in the dispersion curves is their tendency to cross over various branches (Fig. 7). All such points where they cross or repel correspond to some internal

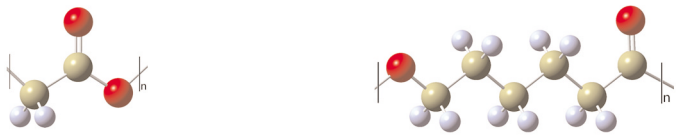

(a) (b)

Fig. 6 (a) One chemical repeat unit of PGA [14]. (b) One chemical repeat unit of PCL [15].

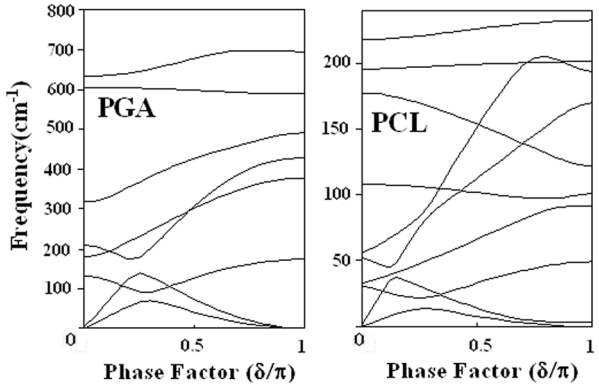

Fig. 7 Low-frequency optical and acoustical modes of PGA and PCL [14].

symmetry point of the polymer chain in the energy momentum space. It implies two different species existing at the same frequency. They have been called "nonfundamental resonances" and are useful in the interpretation of the spectra and interactions involved. When the approaching modes belong to different symmetry species then the two modes can cross over. These crossings are permissible if there is a mirror plane of symmetry.

In PGA, crossing occurs for the pair of modes at (179 and 208 cm^{-1}) and (5 and 133 cm^{-1}). Here we see that the modes that cross over are both dispersive. The interaction of acoustic modes (133 cm^{-1}) at $\delta = 0.167\pi$ and $\delta = 0.386\pi$ can be regarded as an inelastic collision of two phonons in energy momentum space. A similar behavior is observed in the case of PGA and PCL (Figs. 6a and 6b, respectively). A comparison of these low-frequency dispersion curves with PCL shows that although their PED is not the same because of the presence of a different number of methyl groups, but their dispersive behavior is similar. Thus, this profile of dispersion curves appears to be a characteristic of 2-fold aliphatic polyesters, although it needs checking on other macromolecular chains having similar structures. In both of the systems, there are regions of high density-of-states for around the same value of phase factor ($\delta = 0.30\pi$). This is a common feature and an internal symmetry point in both PGA and PCL ($\delta = \pi/6$) [14,15].

The dispersion curves can be used to calculate the heat capacity via density-of-states. A typical heat capacity variation as a function of temperature for PCL is shown in Fig. 8. The agreement with experimental data demonstrates the microscopic and macroscopic agreement in PCL.

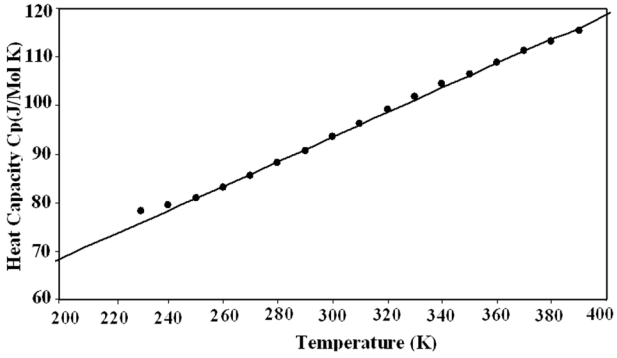

Fig. 8 Heat capacity as a function of temperature for PCL [15]. Solid line: theoretical values; circles: experimental values.

CONDUCTING POLYMERS

This section on conducting polymers is being introduced to demonstrate that dispersion profile reflects not only chain symmetry but also intrachain symmetry. This is obvious from the changes in the dispersion curves in PA when conformational change takes place from the trans to cis state. The conducting polymer that actually launched this new field of research was PA, which in 1974 was accidentally prepared from acetylene as a silver-looking film by Hideki Shirakawa at the Tokyo Institute of Technology in Japan, using Ziegler–Natta-type polymerization catalyst. Conducting polymers are conjugated polymers, namely, organic compounds that have an extended p-orbital system, through which electrons can move from one end of the polymer to the other.

PA has attracted considerable attention because of its quasi-one-dimensional structure and the large range of conductivity possible when doped with electron donors and acceptors. It can reach up to metallic levels. Due to their conjugated structure, PA chains may consist of three possible isomers: cis–transoid (CT), trans–cisoid (TC), and trans–transoid (TT) (Fig. 9a). Here CT and TT isomers are compared.

A comparison of the dispersion curves of the CT and TT forms below 1600 cm^{-1} is given in Fig. 9b. Significant differences are summarized. Since the CT form has a 2-fold symmetry, it has two acoustic modes at zone center and two at $\delta = \pi$. On the other hand, the TT isomer has only translational symmetry and thus has all the acoustic modes at $\delta = 0$. The zone center mode due to ν(C=C), ν(C–C) and φ(C–C–H) appears at 1543 cm^{-1} in CT-PA and 1470 cm^{-1} in the TT form; apart from the energy difference, the dispersion profiles in the two cases are very different. In the former, the energy increases with δ, whereas in the latter, it decreases with increase in δ value. The in-plane bending mode at 1345 and 1247 cm^{-1} in the CT form diverge with increase in δ, whereas the corresponding modes in the TT form, appearing at 1302 and 1235 cm^{-1}, converge and come close at $\delta = \pi$.

The C–H in-phase wagging motion in the CT isomer (assigned at 741 cm^{-1}) and in the TT form (assigned at 1041 cm^{-1}) show similar dispersion profiles. However, the asymmetric CH wags (assigned at 984 cm^{-1} in CT and 887 cm^{-1} in TT) show different profiles. This could be due to an additional contribution in the CT form from C=C torsions [16].

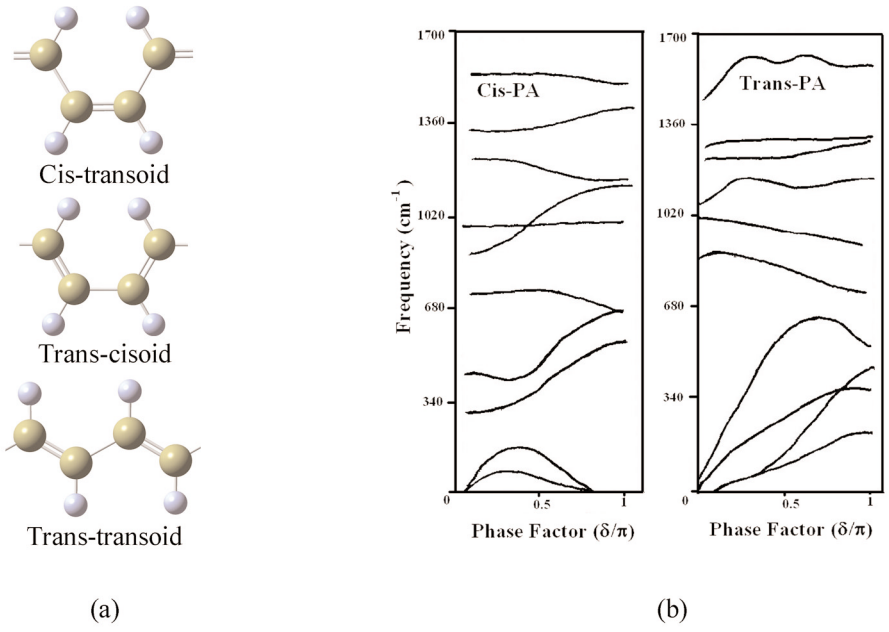

Fig. 9 (a) Isomers of PA. (b) Comparison of dispersion curves of CT and TT PA [16].

CONCLUSION

The symmetry considerations are intimately related to various types of conformations. This is very well brought out in the profile of the dispersion curves especially in the low-frequency optical and acoustical modes.

ACKNOWLEDGMENT

Financial support to PT and DC from the Council of Science and Technology, Uttar Pradesh, India is gratefully acknowledged.

REFERENCES

1. J. Engel, G. Schwarz. *Angew. Chem., Int. Ed. Engl*. **9**, 389 (1970).
2. A. G. Walton, J. Blackwell. *Biopolymers*, Academic Press, New York (1973).
3. G. D. Fasman. *Poly-α-Amino Acids*, Marcel Dekker, New York (1976).
4. V. D. Gupta. *Int. J. Quant. Chem.* **20**, 9 (1981).
5. S. Srivastava, P. Tandon, V. D. Gupta, S. Rastogi, L. Burman, S. B. Katti. *Pramana* **45**, 235 (1995).
6. S. Srivastava, P. Tandon, V. D. Gupta, S. Rastogi, S. B. Katti, C. Mehrotra. *Polym. J.* **29**, 33 (1997).
7. L. Burman, P. Tandon, V. D. Gupta, S. Rastogi. *Polym. J.* **28**, 2389 (1997).
8. P. Tandon, V. D. Gupta, O. Prasad, S. Rastogi, B. Katti. *J. Polym. Sci., Part B: Polym. Phys.* **34**, 1213 (1996).
9. S. Srivastava, P. Tandon, V. D. Gupta, S. Rastogi, S. B. Katti. *Polym. J.* **29**, 492 (1997).
10. N. K. Misra, D. Kapoor, P. Tandon, V. D. Gupta. *Polymer* **41**, 2095 (2000).

11. A. Gupta, P. Tandon, V. D. Gupta, S. Rastogi, G. P. Gupta. *J. Macromol. Sci., Part B: Phys.* **34**, 401 (1995).
12. L. Burman, P. Tandon, V. D. Gupta, S. Srivastava. *J. Macromol. Sci., Part B: Phys.* **34**, 379 (1995).
13. L. Burman, P. Tandon, V. D. Gupta, S. Rastogi, S. Srivastava. *Biopolymers* **38**, 53 (1996).
14. R. Agarwal, R. M. Misra, P. Tandon, V. D. Gupta. *Polymer* **45**, 5307 (2004).
15. R. M. Misra, R. Agarwal, P. Tandon, V. D. Gupta. *Eur. Polym. J.* **40**, 1787 (2004).
16. A. Kumar, S. Pande, P. Tandon, V. D. Gupta. *J. Macromol. Sci., Part B: Phys.* **39**, 303 (2000).
17. D. Jacquemin, J.-M. Andre, B. Champagne. *J. Chem. Phys.* **118**, 3956 (2003).
18. N. J. Ramer, T. Marrone, K. A. Stiso. *Polymer* **47**, 7160 (2006).
19. K. Honda, Y. Furukawa, H. Nishide. *Vib. Spectrosc.* **40**, 149 (2006).
20. S. Lakard, G. Herlem, B. Lakard, B. Fahys. *J. Mol. Struct. (Theochem)* **685**, 83 (2004).
21. M. Kaledin, A. Brown, A. L. Kaledin, J. M. Bowman. *J. Chem. Phys.* **121**, 5646 (2004).
22. E. Henssge, D. Dumont, D. Fischer, D. Bougeard. *J. Mol. Struct.* **482–483**, 491 (1999).
23. R. H. Boyd, R. H. Gee, J. Han, Y. Jin. *J. Chem. Phys.* **101**, 789 (1994).
24. S. Neyertz, D. Brown, J. O. Thomas. *J. Chem. Phys.* **101**, 10064 (1994).
25. C. E. Wozny, B. G. Sumpter, D. W. Noid. *J. Chem. Phys.* **100**, 3520 (1994).
26. D. Dumont, E. Henssge, D. Ficher, D. Bougeard. *Macromol. Theory Simul.* **7**, 373 (1998).
27. D. Dumont, D. Bougeard. *Comput. Theo. Polym. Sci.* **9**, 89 (1999).
28. S. Nakamura, M. Ikeguchi, K. Shimizu. *Chem. Phys. Lett.* **372**, 423 (2003).
29. V. N. Kabadi, B. M. Rice. *J. Phys. Chem. A* **108**, 532 (2004).
30. E. B. Wilson Jr. *J. Chem. Phys*. **9**, 76 (1941).
31. E. B. Wilson, J. C. Decius, P. C. Cross. *Molecular Vibrations*, McGraw-Hill, New York (1955).
32. E. P. Wigner. *Group Theory and its Application to the Quantum Mechanics of Atomic Spectra*, Academic Press, New York (1959).
33. P. W. Higgs. *Proc. R. Soc. (London)* **A220**, 472 (1953).
34. E. Wodewig. *Matrix Calculus*, North-Holland, Amsterdam (1959).
35. H. Tadokaro. *J. Chem. Phys*. **33**, 1558 (1960).
36. C. Y. Liang, S. Krimm, G. B. B. M. Sutherland. *J. Chem. Phys.* **25**, 543 (1953).
37. S. Krimm, C. Y. Liang, G. B. B. M. Sutherland. *J. Chem. Phys.* **25**, 549 (1956).
38. C. Y. Liang, S. Krimm. *J. Chem. Phys.* **25**, 563 (1956).
39. C. Y. Liang, S. Krimm. *J. Polym. Sci.* **24**, 241 (1958).
40. C. Y. Liang, S. Krimm. *J. Mol. Spectrosc.* **3**, 554 (1959).
41. S. Krimm, C. F. Liang. *J. Polym. Sci.* **22**, 95 (1956).
42. S. Krimm. *Fortschr. Hochpolymer-Forsch*. **2**, 51 (1960).
43. L. Piseri, G. Zerbi. *J. Chem. Phys.* **48**, 3561 (1968).
44. H. C. Urey, H. C. Bradley. *Phys. Rev*. **38**, 1969 (1931).
45. W. Qian, N. G. Mirikin, S. Krimm. *Chem. Phys. Lett*. **315**, 125 (1999).
46. T. H. Benzinger. *Nature* **229**, 100 (1971).
47. R. Pan, M. Verma-Nair, B. Wunderlich. *J. Therm. Anal*. **35**, 955 (1989).
48. K. A. Roles, A. Xenopoulos, B. Wunderlich. *Biopolymers* **33**, 753 (1993).
49. P. W. Atkins, R. S. Friedman. *Molecular Quantum Mechanics*, 3rd ed., Oxford University Press, Oxford (2001).
50. P. Hohenberg, W. Kohn. *Phys. Rev. B* **136**, 864 (1964).
51. W. Kohn, L. J. Sham. *Phys. Rev. A* **140**, 1133 (1965).
52. J. C. Slater. *Quantum Theory of Molecules and Solids*, Vol. 4, McGraw-Hill, New York (1974).
53. S. H. Vosko, L. Wilk, M. Nasair. *Can. J. Phys*. **58**, 1200 (1980).
54. B. Miehlich, A. Savin, H. Stoll, H. Preuss. *Chem. Phys. Lett*. **157**, 200 (1989).
55. C. Lee, W. Yang, R. G. Parr. *Phys. Rev. B* **37**, 785 (1988).
56. A. D. Becke. *Phys. Rev. A* **38**, 3098 (1988).
57. J. P. Perdew, W. Wang. *Phys. Rev. B* **45**, 13244 (1992).

58. R. G. Parr, W. Young. *Density Functional Theory of Atoms and Molecules*, Oxford University Press, New York (1989).
59. G. D. Fasman, K. Itoh, C. S. Liu, R. C. Lord. *Biopolymers* **17**, 125 (1978).